Boundary-Layer Flows from Fixed to Moving Surfaces Including Gap Effects

J. S. Tennant*
Florida Atlantic University, Boca Raton, Fla.

W. S. Johnson†
University of Tennessee, Knoxville, Tenn.
and
D. D. Keaton‡
General Dynamics Corp., Ft. Worth, Tex.

This paper reports a study that analyzes a moving wall as a boundary-layer control device. The moving wall, normally the surface of a rotating cylinder, is located in a region of high adverse pressure gradient and energizes the boundary layer in an effort to delay or prevent flow separation. A numerical model based on the method of Cebeci and Smith is presented for the region of flow from the fixed wall, through the transition region, and onto the moving surface. Numerical results are presented showing excellent agreement with available data. Parametric studies are also undertaken to show the predicted effects of the ratio of wall velocity to freestream velocity and the gap between the fixed and moving surfaces at the transition point.

Nomenclature

U = local x-direction velocity
V = local y-direction velocity
U_e = local freestream velocity
U_0 = velocity of the moving surface
U_∞ = undisturbed freestream velocity
$\overline{u'v'}$ = turbulent shear stress
U_* = friction velocity $(\tau_0/\rho)^{1/2}$
x = boundary layer coordinate along the body
y = boundary layer coordinate normal to the body
ϵ = eddy viscosity
δ = boundary layer thickness
δ^* = displacement thickness
β = ratio of moving wall velocity to freestream velocity
λ = acceleration length
ζ = distance along moving surface from termination of fixed wall

Introduction

NEWTON first observed the effects of moving wall boundary-layer control upon the path traveled by a spinning ball.[1] However, at that time nothing was known of the details of the effect. Almost 200 years later, Rayleigh and Magnus studied the effect of spinning a cylinder exposed to a stream flow and noted the lift.[1] Flettner[2] later used this effect to construct a ship with a vertical rotating cylinder replacing the usual sail. In 1934, Goldstein[3] illustrated the principle of boundary-layer control using a rotating cylinder at the leading edge of a flat plate. One of the most practical direct applications of moving wall boundary-layer control was made in 1936 by Farve.[4] In Farve's experiment he replaced the upper surface of an airfoil with an endless moving band and illustrated that the boundary layer could be controlled and the airfoil could be operated at very high angles of attack. However, the mechanical difficulties of using such an airfoil have prevented its use.

One of the modern developments making practical use of moving wall boundary-layer control is that reported in 1961 by Alvarez-Calderon and Arnold.[5] They located a rotating cylinder at the junction of an airfoil and the trailing edge flap to provide a high lift airfoil for STOL-type aircraft. Alvarez-Calderon and Arnold designed their airfoil based on a lengthy series of experimental tests and reported no detailed study of the boundary-layer phenomenon.

Brooks[6] conducted water tunnel tests on a hydrofoil with a rotating cylinder both in the leading edge and at the trailing edge and reported lift as a function of cylinder speed. The trailing-edge cylinder produced a significant increase in lift at zero angle of attack while the leading-edge cylinder produced no effect, since the Kutta condition was maintained due to the sharp trailing edge.

A recent advancement in ship control is the development of the "super rudder" by B. N. Steele of Britain's National Physical Laboratory.[7] This rudder operates on the principle of boundary-layer control provided by a rotating cylinder at the leading edge. Although this is a simple modification of the conventional rudder, the performance is vastly improved with unseparated flow extended from a 35-deg unseparated angle of the conventional rudder to angles in excess of 70 deg.

Moving walls have been used in internal flow by Tennant[8] to control the boundary-layer development along the walls of a diffuser. The diffuser used sections of rotating cylinders for walls, and, by operating the cylinders at surface speeds greater than the fluid velocities, boundary-layer control was attained. The diffuser was very successful and provided unseparated flows for area ratios of up to 2.5:1 with overall length approximately equal to the exit channel width. Tennant provided a detailed computer analysis of the boundary layer using a numerical calculation procedure and had good success in predicting diffuser performance.

The region of transition from the fixed wall to the moving wall, as shown schematically in Fig. 1, is a region where two boundary-layer flows merge into a single boundary-layer flow on a moving surface. Tennant[9] relied on an artifice to model this region, and ignored the physical gap between surfaces by assuming all of the acceleration effect of the wall occurred in a fixed streamwise span, λ (see Fig. 2). By allowing the

Received July 6, 1977; revision received Oct. 19, 1977.

Index categories: Boundary Layers and Convective Heat Transfer – Turbulent; Hydrodynamics.

*Associate Professor of Ocean Engineering. Member AIAA.
†Professor of Mechanical and Aerospace Engineering. Member AIAA.
‡Research Engineer. Associate Member AIAA.

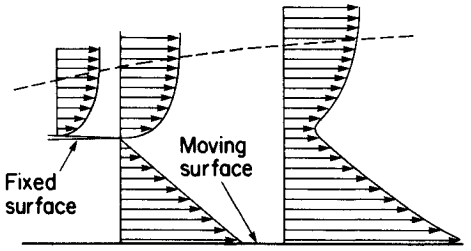

Fig. 1 Flow model at the fixed-moving wall transition.

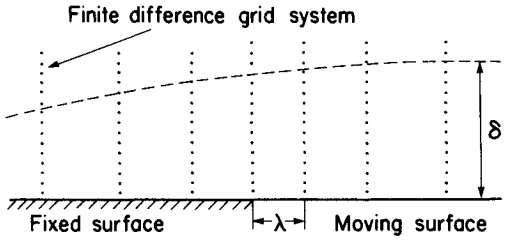

Fig. 2 Previous flow model at the fixed-moving wall transition.

numerical calculation procedure to make a step length λ, he found that satisfactory calculations could proceed streamwise; this method was verified by a small amount of experimental data. In particular, Tennant found the value of λ for adequate calculations to be equal to the boundary-layer thickness.

The purpose of this paper is to present a more realistic model of the flow from the fixed surface to a moving surface using many ideas from Tennant's model, but accounting for the inevitable physical gap that must exist between fixed and moving surfaces in any physically realizable situation. This model was then used for calculations of moving wall boundary layers and a comparison was made with new moving wall experimental data as reported herein.

Analytical Model

Consider the physical situation as shown in Fig. 1. The fixed forward surface with a sharp trailing edge is followed by a moving surface (usually a rotating cylinder). The gaps to be considered are somewhat less than the thickness of the boundary layer approaching along the fixed surface. In order to achieve a phenomenological model, a velocity profile as illustrated in Fig. 1 was assumed, i.e., classical boundary-layer flow on the upper fixed surface with laminar Couette flow in the gap region. These flows leave a fixed surface and join to form the downstream flow along the moving wall.

Tennant[9] considered the use of the three boundary-layer computer simulation programs (Smith-Clutter, Herring-Mellor, Cebeci-Smith); the latter two receiving a "good" rating from the Stanford Conference of 1968.[10] The method, as described by Cebeci and Smith,[11] was chosen for adaption to the moving wall condition because of its use of a variable spaced grid and unique integration technique. An outline of the Cebeci-Smith method as modified by Tennant follows.

For two-dimensional flow, the appropriate governing equations are continuity and the x-momentum equation.

$$\frac{\partial U}{\partial x}+\frac{\partial V}{\partial y}=0$$

$$U\frac{\partial U}{\partial x}+V\frac{\partial U}{\partial y}=U_e\frac{dU_e}{dx}+\nu\frac{\partial^2 U}{\partial y^2}-\frac{\partial}{\partial y}(\overline{u'v'})$$

For the fixed wall case, boundary conditions are given by $U(x,0)=0$, $V(x,0)=0$, and $U(x,\delta)=U_e(x)$. However, for

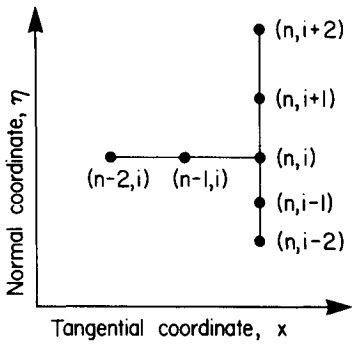

Fig. 3 Finite difference node system for the node (n,i).

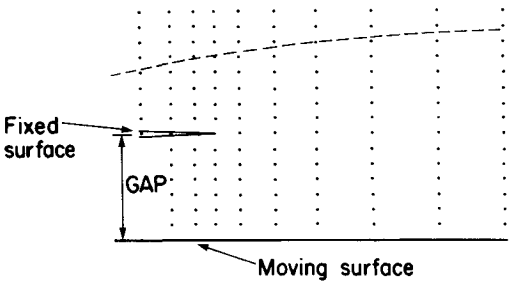

Fig. 4 Nodal distribution near the fixed-moving wall transition.

the case of moving walls, the first boundary condition may be changed to $u(x,0)=U_0$, where U_0 denotes the surface velocity at x. The technique uses a two-layer eddy viscosity model to eliminate the Reynolds shear stress term in the momentum equation. The two-layer model uses an inner layer model as suggested by Clauser as

Inner layer

$$\epsilon_i=k^2y^2\left\{1-\exp\left[\frac{-y}{26\nu}\left(\frac{\psi_w}{\rho}+\frac{dp}{dx}\frac{y}{\rho}\right)^{1/2}\right]\right\}^2\left|\frac{\partial U}{\partial y}\right|$$

Outer layer

$$\epsilon_0=k_1U_e\delta^*$$

Tennant[9] modified the expression for the outer eddy viscosity for the case of wall motion as $\epsilon_0=k_2U_*\delta$.

The Van Driest model for ϵ_i is particularly well suited for this application since it makes use of the absolute value of the velocity gradient. As will be seen in the results that follow, the velocity gradient in the vicinity of the wall will be negative along the moving walls. Since the displacement thickness δ^* is strongly influenced by wall motion and can even become negative at large values of β, a modification to the outer layer model was required to keep it independent of the inner region behavior. This model was verified and the constant k_2 was evaluated by performing boundary-layer calculations for several fixed-wall configurations. The equations are then transformed by use of the Blasius transformations

$$x=x;\ \eta=y(U_e/\nu x)^{1/2},\ \text{and}\ \psi(x,y)=[\nu x U_e(x)]^{1/2}f(x,\eta)$$

Incorporation of a variable grid and the associated expressions for the derivatives in the normal boundary-layer coordinate direction along with linearizing the equations on the tangential boundary-layer coordinate direction allows the momentum equation to be reduced to a set of N equations and N unknowns for N grid points lying across the boundary layer of the form

$$\Delta\phi_{i+2}+F_i\overline{\Delta\phi_{i+1}}+G_i\overline{\Delta\phi_i}+I_i\overline{\Delta\phi_{i-1}}+M_i\overline{\Delta\phi_{i-2}}=N_i$$

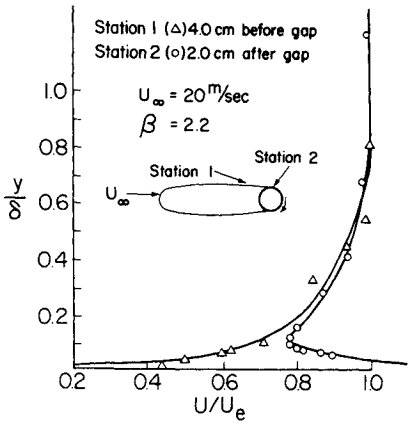

Fig. 5 Measured and calculated boundary-layer velocity profiles for both fixed and moving wall layers (gap = 0.12 cm).

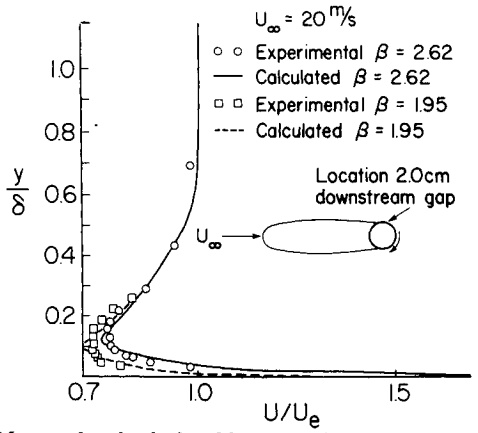

Fig. 6 Measured and calculated boundary-layer velocity profiles for moving wall boundary layers at different wall velocities (gap = 0.08 cm).

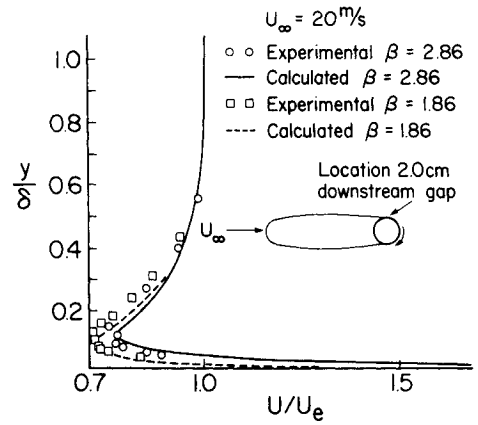

Fig. 7 Measured and calculated boundary-layer velocity profiles for moving wall boundary layers at different wall velocities (gap = 0.04 cm).

where $\Delta\phi$ is a change in the transformed stream function $\phi = f - \eta$ at a particular grid point. Figure 3 shows a finite difference nodal system at grid point (n,i) for the method. Notice that the ratio of the distances between successive grid points across the boundary layer equals a constant. A set of equations described by the preceding general equation was written and solved at a station of concern in a stepwise manner along the surface of concern.

The grid system for the numerical calculations including the step in the wall is shown in Fig. 4. Since the Cebeci-Smith solution is dependent on three previous stations for the next streamwise velocity profile calculation, only three positions in the "gap" area were used. Following an assumption of

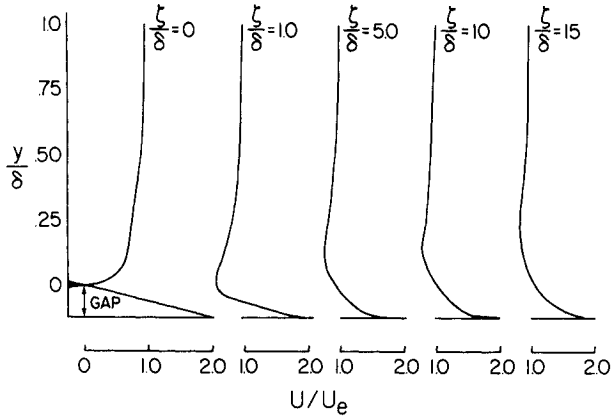

Fig. 8 Development of the boundary-layer velocity profile downstream of the fixed-moving wall transition (β = 2.0).

laminar Couette flow (verified by Reynolds number calculation in the gap), with no pressure gradient in the gap, a linear velocity profile was assumed with zero velocity at the top of the gap and a velocity equal to that of the moving surface at the bottom. Once the moving wall portion of the boundary layer is reached in the calculation process, Tennant's model for inner layer eddy viscosity is used assuming a step increase in boundary-layer thickness equal to the gap size. Since information on the rate of transition of the laminar gap flow into turbulent flow was not available, it was assumed the turbulence was introduced immediately and the calculation at the first station downstream of the gap was made assuming a fully turbulent boundary layer. This calculation station was one boundary-layer thickness downstream of the gap.

Results

Comparison with Experimental Data

A boundary-layer flow from a fixed to moving surface used for comparison was measured on a body as shown in Fig. 5 and is reported by Tennant, et al.[12] Data were taken using a precision traverse mechanism and a boundary-layer total pressure probe. Figure 5 illustrates experimental data and results of calculations using the method described at a location upstream of the gap on the fixed surface and a single station on the moving wall. The fixed wall profile clearly shows that conditions upstream of the gap are suitably modeled. Figures 6 and 7 give other comparisons with data at various values of β, the nondimensional wall velocity.

The calculations were made based upon boundary layer transition from laminar to turbulent flow at a momentum thickness Reynolds number of 360. This places all the boundary layers shown in the turbulent regime. Boundary-layer calculations were initiated from an exact solution for stagnation point flow at a stagnation point measured by the "moving tuft" method described by Tennant et al.[13] The pressure distribution for the flow was provided by a static wall pressure measurement and a subsequent potential flow solution to cover flow over the moving surface.

Effects of Gap and Wall Velocity

The model was employed to show, in a more generalized case, the gap and wall velocity effects on the boundary-layer velocity profiles on the moving wall. A flat-plate geometry was chosen for these calculations to eliminate the effects of pressure gradient on the gap and surface velocity effects. The flow of air at standard conditions and a freestream velocity of 30 m/s was analyzed. The gap was located at the point where the Reynolds number based on momentum thickness was 1700, well into the turbulent boundary-layer regime.

Figure 8 shows the development of the boundary-layer velocity profile from the downstream location of the gap, a distance of approximately 15 boundary-layer thicknesses

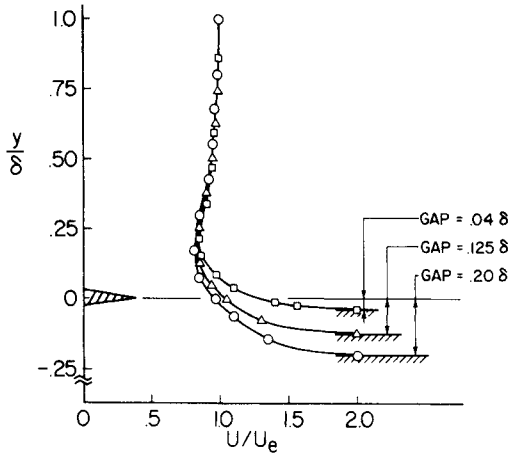

Fig. 9 Predicted effect of the gap on the boundary-layer velocity profile at $\zeta = 15\delta$.

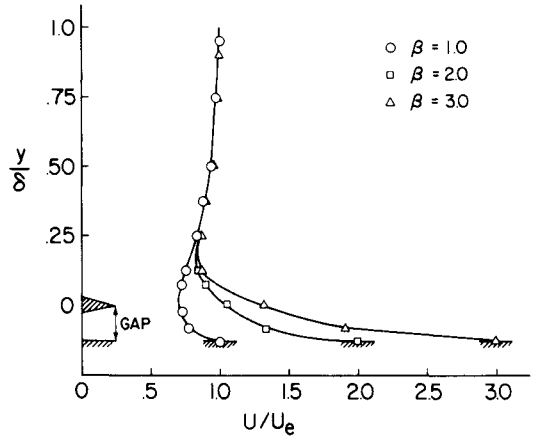

Fig. 10 Predicted effect of the wall velocity on the boundary-layer velocity profile at $\zeta = 15\delta$.

(about 0.15 m). An important feature of the flowfield is the rapid acceleration that occurs along the streamline where the gap flow merges with the main boundary-layer flow. This illustrates the effectiveness of the moving wall as a momentum transport device.

Figure 9 illustrates the effect of the gap size on the velocity profile at a location 15 boundary-layer thicknesses downstream of the gap. The smaller gaps give slightly higher velocities in the boundary layer, indicating at least some potential improvement in boundary-layer control for smaller gaps.

Figure 10 shows the effect of wall velocity on the boundary layer and, as expected, this is the most significant parameter to be considered. For example, at a velocity ratio β of 3, the minimum layer velocity has increased from zero at the gap to nearly 85% of the freestream value in a distance of 15 boundary-layer thicknesses.

Conclusions

The analytical model represents a significant improvement over past calculation techniques. It is now possible to include gap size as a parameter in a moving wall boundary-layer model without reliance on an acceleration length. The comparisons of experimental data and calculation show that excellent results can be achieved using this method. It should be emphasized that the model is only applicable where the junction of the moving and fixed walls is such that the fixed wall ends with a very sharp trailing edge and the flow situation is such that the Couette flow from the gap and the fixed wall boundary-layer flow join in a smooth parallel flow.

Acknowledgment

This work was sponsored by the U. S. Navy Ship Research and Development Center, Contract no. N00014-71-A-0121-006.

References

[1] Thwaites, B., ed., *Incompressible Aerodynamics*, Clarendon Press, Oxford, England, 1960, p. 215.

[2] Prandtl, L., *Essentials of Fluid Dynamics*, Hafner Publishing Co., New York, 1952, p. 71.

[3] Goldstein, S., ed., *Modern Developments in Fluid Dynamics*, Clarendon Press, Oxford, England, 1938, p. 78.

[4] Farve, M. A., "Un Nouveau Procede Hypersustentateur: L'aile a' Parol d'Extrados Mobile," *Mechanique Experimentale Des Fluids*, Comtes Rendus, 1934, p. 634.

[5] Alvarez-Calderon, A. and Arnold, F. R., "A Study of the Aerodynamic Characteristics of a High-Lift Device Based on a Rotating Cylinder Flap," Stanford University Tech. Rept. RCF-1, 1961.

[6] Brooks, J. D., "The Effect of a Rotating Cylinder at the Leading and Trailing Edges of a Hydrofoil," U.S. Naval Ordnance Test Station, NAVWEPS Rept. 8042, China Lake, Calif., April 1963.

[7] Steele, B. N. and Harding, M. H., "The Application of Rotating Cylinders to Ship Maneuvering," National Physical Laboratory (Britain) Ship Rept. 148, Dec. 1970.

[8] Tennant, J. S., "A Subsonic Diffuser with Moving Walls for Boundary Layer Control," *AIAA Journal*, Vol. 11, Feb. 1973, p. 240.

[9] Tennant, J. S. and Yang, T., "Turbulent Boundary Layer Flows from Stationary to Moving Surfaces," *AIAA Journal*, Vol. 11, Aug. 1973, pp. 1156-1161.

[10] Kline, S. J., Cockrell, D. J., Morkovin, M. V., and Sovran, G., "Proceedings on Computation of Turbulent Boundary Layers," Vol. 1, Dept. of Mechanical Engineering, Stanford Univ., Stanford, Calif., Aug. 1968.

[11] Cebeci, T. and Smith, A.M.O., "A Finite Difference Solution of the Incompressible Turbulent Boundary Layer Equations by an Eddy Viscosity Concept," McDonnel Aircraft Co., Rept. No. DAC-67130, Oct. 1968.

[12] Tennant, J. S., Johnson, W. S. and Krothapalli, A., "A Rotating Cylinder for Circulation Control on an Airfoil," *Journal of Hydronautics*, Vol. 10, No. 3, July 1976, pp. 102-105.

[13] Tennant, J. S., Johnson, W. S. and Krothapalli, A., "Moving Tuft Method for Stagnation Point Location," *Journal of Aircraft*, Vol. 13, Jan. 1976, pp. 61-62.